Monthly Notices
of the
ROYAL ASTRONOMICAL SOCIETY

MNRAS **454,** 4467–4475 (2015) doi:10.1093/mnras/stv2276

Is 4U 0114+65 an eclipsing HMXB?

Pragati Pradhan,[1,2⋆] Biswajit Paul,[3⋆] B. C. Paul,[2] Enrico Bozzo[4⋆] and Tomaso M. Belloni[5]

[1]*St. Joseph's College, Singamari, Darjeeling 734104, West Bengal, India*
[2]*North Bengal University, Raja Rammohanpur, District Darjeeling 734013, West Bengal, India*
[3]*Raman Research Institute, Sadashivnagar, Bangalore 560080, India*
[4]*ISDC, University of Geneva, Chemin d'Ecogia 16, CH-1290 Versoix, Switzerland*
[5]*INAF Osservatorio Astronomico di Brera, Via E Bianchi 46, I-23807 Merate (LC), Italy*

Accepted 2015 September 28. Received 2015 September 26; in original form 2015 August 4

ABSTRACT

We present the pulsation and spectral characteristics of the High-Mass X-ray Binary (HMXB) 4U 0114+65 during a *Suzaku* observation covering the part of the orbit that included the previously known low-intensity emission of the source (dip) and the egress from this state. This dip has been interpreted in previous works as an X-ray eclipse. Notably, in this *Suzaku* observation, the count rate during and outside the dip vary by a factor of only 2–4 at odds with the eclipses of other HMXBs, where the intensity drops up to two orders of magnitude. The orbital intensity profile of 4U 0114+65 is characterized by a narrow dip in the *RXTE*-ASM (2–12 keV) light curve and a shallower one in the *Swift*-BAT (15–50 keV), which is different from eclipse ingress/egress behaviour of other HMXBs. The time-resolved spectral analysis reveal moderate absorption column density ($N_{\rm H}$ – 2–20 × 10^{22} atoms cm^{-2}) and a relatively low equivalent width (∼30 and 12 eV of the iron Kα and Kβ lines, respectively) as opposed to the typical X-ray spectra of HMXBs during eclipse where the equivalent width is ∼1 keV. Both X-ray Imaging Spectrometer and HXD-PIN data show clear pulsations during the dip, which we have further confirmed using the entire archival data of the IBIS/ISGRI and JEM-X instruments onboard *INTEGRAL*. The results we presented question the previous interpretation of the dip in the light curve of 4U 0114+65 as an X-ray eclipse. We thus discuss alternative interpretations of the periodic dip in the light curve of 4U 0114+65.

Key words: pulsars: general – X-rays: binaries – X-rays: individual: 4U 0114+65.

1 INTRODUCTION

The hard X-ray source 4U 0114+65 (alias 2S 0114+650) is a pulsar belonging to a class of persistent High-Mass X-ray Binaries (HMXBs), showing properties similar to both Be (Koenigsberger et al. 1983) and supergiant X-ray binaries Crampton, Hutchings & Cowley (1985); Reig et al. (1996). It was discovered in the *SAS-3* galactic survey (Dower et al. 1977). The pulsar's companion is a B1Ia supergiant (LS I+65 010) located at a distance of ∼7.2 kpc (Reig et al. 1996). From the optical radial velocity measurements, Crampton et al. (1985) first confirmed the binary nature of 4U 0114+65. By assuming an eccentricity of ∼0.16, these authors estimated an orbital period of ∼11.588 d. The corresponding value in case of a circular orbit is ∼11.591 d. Similar values of the system orbital period have also been reported in later works: Corbet, Finley & Peele (1999) obtained an X-ray variability of ∼11.63 d from the *RXTE*-ASM observations carried out between 1996 and 1999; Wen et al. (2006) reanalysed ASM data from 1996 to 2004 and obtained an orbital period of ∼11.599 d; Grundstrom et al. (2007) obtained an orbital period of ∼11.5983 d by using both optical and X-ray observations. These authors also reported an eccentricity of the orbit of ∼0.18.

A stable 2.78 h periodicity in the X-ray light curve of the source was first reported by Finley, Belloni & Cassinelli (1992) by using *EXOSAT* and *ROSAT* data. A similar modulation was also observed in the optical by Taylor et al. (1995). Corbet et al. (1999) and Hall et al. (2000) further confirmed the same periodicity by analysing the *RXTE*-ASM and PCA data, respectively. Additional X-ray observations proved that the periodicity at 2.7 h was getting faster over time, firmly establishing its association with the spin period of the neutron star hosted in this system (Hall et al. 2000; Bonning & Falanga 2005; Farrell et al. 2008). This is one of the slowest pulsar known and various models have been proposed to explain its unusually long spin period (Hall et al. 2000 and references therein). Li & van den Heuvel (1999) suggested that such long spin period could

⋆ E-mail: pragati2707@gmail.com (PP); bpaul@rri.res.in (BP); Enrico.Bozzo@unige.ch (EB)

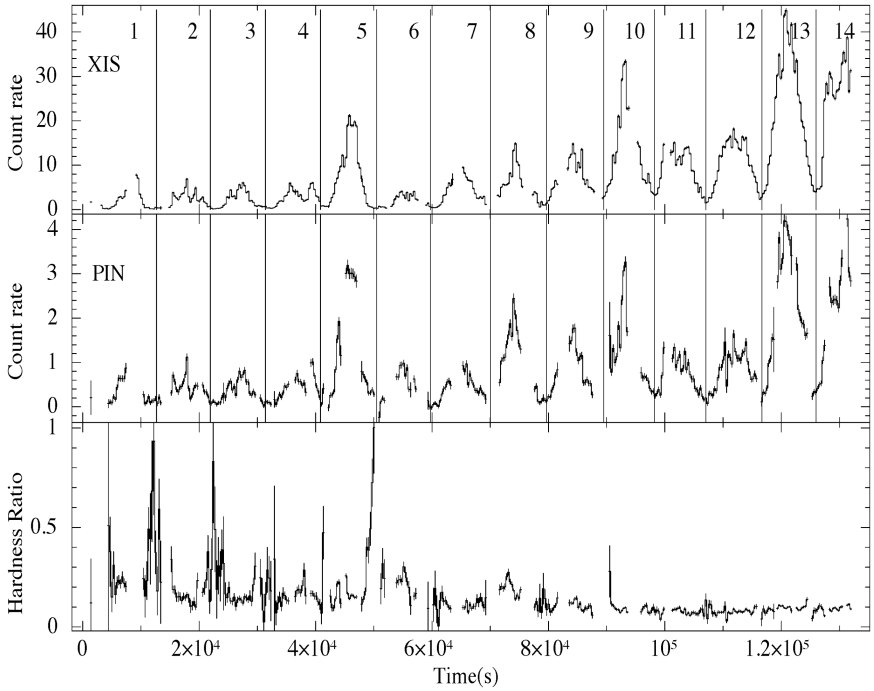

Figure 1. Background subtracted *Suzaku* light curves of 4U 0114+65. The time bin is 300 s. The upper and middle panels show the XIS and HXD-PIN data, respectively. The hardness ratio of the XIS and HXD-PIN data is reported in the bottom panel. The start time of the light curves is 55763.4805 MJD.

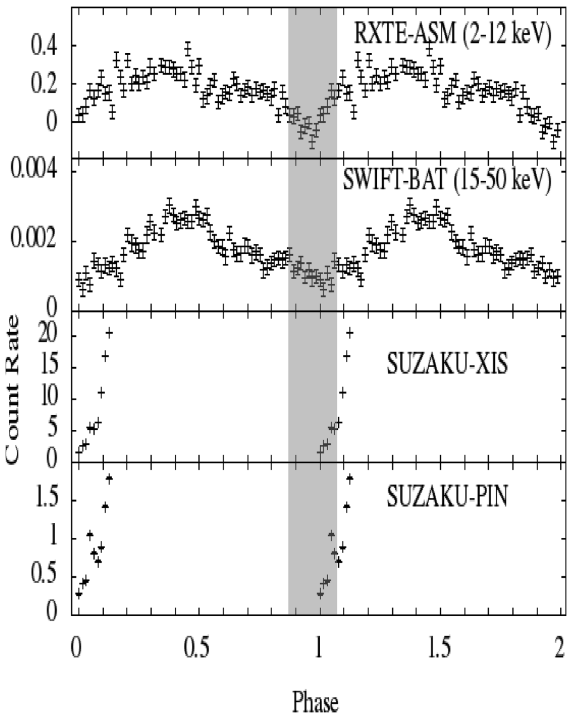

Figure 2. Light curves of *RXTE*-ASM, *Swift*-BAT, XIS and HXD-PIN folded at the orbital period of 4U 0114+65 (the initial epoch is chosen to be MJD 55763.4805). A complete eclipse is detected only in the ASM data, which covers a softer X-ray energy range than BAT. (Note that the negative count rate in the ASM data is only apparent which arises from the automated background subtraction of the ASM light curve and correspond to the time when the source was too faint to be detected by it). The shaded region shows the ingress and egress time of the dip (as seen in the ASM data) lasting for nearly one day each.

be achieved if the neutron star was initially born as a magnetar. The possible cyclotron resonant absorption features at ∼22 and 44 keV reported by Bonning & Falanga (2005) did not provide support in favour of this hypothesis, as they would imply a magnetic field of $\sim 2.5 \times 10^{12}$ G for the pulsar in 4U 0114+65. However, subsequent observations did not confirm the detection of the cyclotron features (den Hartog et al. 2006; Masetti et al. 2006; Farrell et al. 2008).

4U 0114+65 shows a remarkable variability in X-rays, with aperiodic flares lasting for a few hours (Yamauchi et al. 1990; Apparao, Bisht & Singh 1991) and short-term flickering occurring on timescales of minutes (Koenigsberger et al. 1983). A superorbital modulation of ∼30.7 d has been detected in *RXTE*-ASM data (Farrell, Sood & O'Neill 2006; Wen et al. 2006), and found to be stable over time. This makes 4U 0114+65 the fourth system to show stable superorbital variability (see also the cases of SMC X-1, Her X-1, LMC X-4 and SS 433; Sood et al. 2006).

The orbital intensity profile of 4U 0114+65 as obtained from the *RXTE*-ASM shows a dip that has been usually associated with an X-ray eclipse. Here, we report on the timing and broad-band spectral characteristics of the X-ray emission from 4U 0114+65 as observed with *Suzaku* during part of the dip and the dip egress. The *Suzaku* observation indicates that the X-ray emission from the source recorded during the dip is not compatible with what is usually observed from an HMXB in eclipse. In order to gain further insights on the nature of the dip, we thus also looked at the pulsation characteristics of this source by using all publicly available IBIS/ISGRI and JEM-X data from the *INTEGRAL* satellite.

2 OBSERVATION AND ANALYSIS

2.1 *Suzaku*

Suzaku (Mitsuda et al. 2007) is a broad-band X-ray observatory which covers the energy range of 0.2–600 keV. It has two main

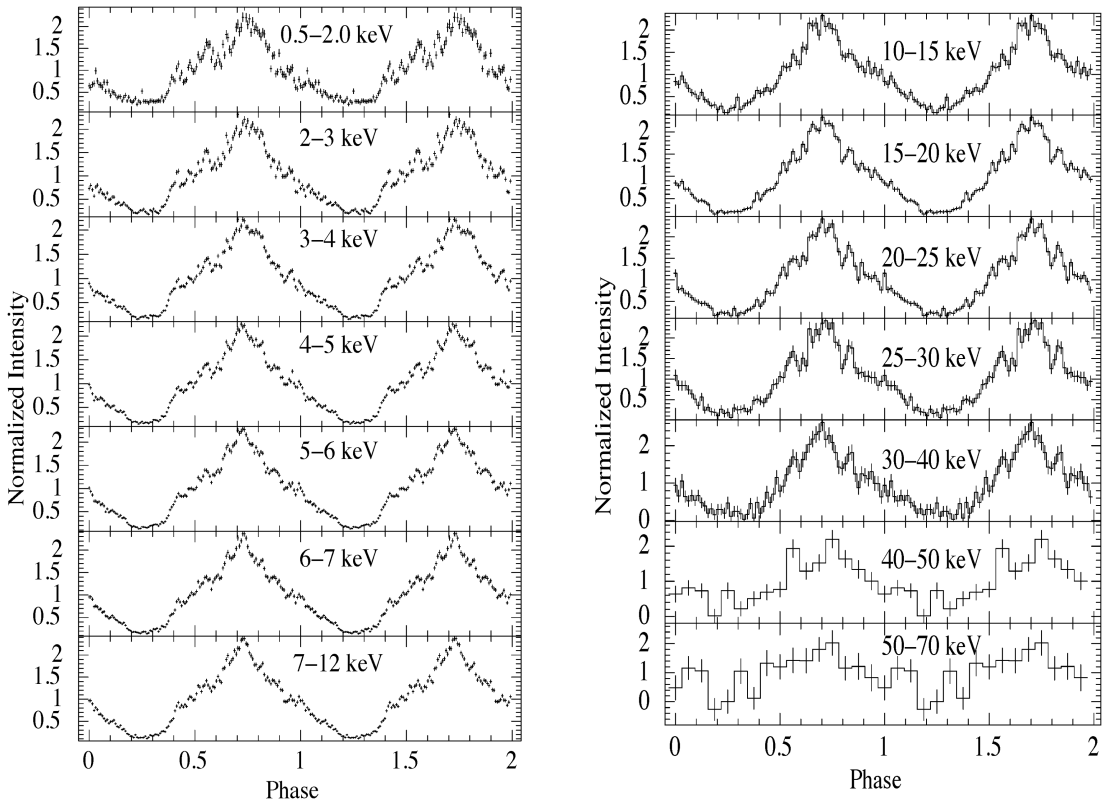

Figure 3. The left- and right-hand panels show the energy-resolved pulse profiles of the XIS and HXD-PIN, respectively. We used a spin period of 9391.19 s and an initial epoch TJD (Truncated Julian Date) 15763. The pulse profiles do not show any obvious energy dependence.

instruments: the X-ray Imaging Spectrometer (XIS; Koyama et al. 2007), covering the 0.2–12 keV energy range, and the Hard X-ray Detector (HXD). The latter comprises HXD-PIN diodes (Takahashi et al. 2007), covering the 10–70 keV energy range, and GSO crystal scintillator detectors, covering the 70–600 keV energy range. The XIS consists of four CCD detectors of which three are front illuminated (FI) and one is back illuminated (BI). Only three out of the four XIS units (XIS 0,1 and 3) are currently operational.

4U 0114+65 was observed with *Suzaku* on 2011 July 21 and 22 (OBSID '406017010'). The observation was carried out at the 'XIS nominal' pointing position and the effective exposure time of the XIS and HXD-PIN was of 106.5 and 88.5 ks, respectively. The XIS units were operated in 'standard' data mode with the 'Window 1/4' option (providing a time resolution of 2 s).

For the XIS and HXD data, we used the filtered cleaned event files which are obtained using the pre-determined screening criteria as suggested in the *Suzaku* ABC guide.[1] XIS light curves and spectra were extracted from the XIS data by choosing circular regions of 3 arcmin radius from the source position. Background light curves and spectra for the XIS were extracted by selecting regions of the same size in a portion of the CCD that did not contain any source photons. For the HXD-PIN, simulated 'tuned' non-X-ray background (NXB) event files corresponding to the month and year of the respective observations were used to estimate the NXB[2] (Fukazawa et al. 2009).

The timing analysis of the *Suzaku* data was performed on the XIS and HXD-PIN light curves after applying barycentric corrections to the event data files (we used the FTOOLS task 'AEBARYCEN'). These files were also corrected for dead time effects by using the FTOOLS task 'HXDDTCOR'. Light curves were extracted from the XIS data with the highest available time resolution of 2 s. We summed the background subtracted XIS 0, 1 and 3 light curves and obtained a single background-corrected light curve for all the XIS units. The HXD-PIN light curves were extracted with a resolution of 1 s and the corresponding background was evaluated by generating similar light curves from the simulated background files.

The XIS and HXD-PIN light curves comprise 14 neutron-star rotations, as shown in Fig. 1. The average source count rate in the two instruments was 2.69 c s^{-1} and 0.85 c s^{-1}, respectively.

The XIS spectra were extracted with 2048 channels and the HXD-PIN spectra with 255 channels. Response files for the XIS were created using CALDB version '20140701'. For the HXD-PIN spectrum, response files corresponding to the epoch of the observation were obtained from the *Suzaku* guest observer facility.[3]

2.1.1 *Timing Analysis*

The source HXD-PIN and XIS light curves are reported in Fig. 1 (the bin size is 300 s). The upper and middle panel of the figure show the XIS and HXD-PIN data, respectively. The lower panel show the hardness ratio between the HXD-PIN and XIS. Pulsations can be clearly seen even during the lowest X-ray emission time interval, i.e. the dip. The average count rates measured during dip and out of the dip differ only by a factor of ∼2–4.

[1] http://heasarc.gsfc.nasa.gov/docs/suzaku/analysis/abc/
[2] http://heasarc.nasa.gov/docs/suzaku/analysis/pinbgd.html
[3] http://heasarc.nasa.gov/docs/heasarc/caldb/suzaku/

Table 1. Best-fitting parameters of the time-averaged spectra of 4U 0114+65 for different models extracted from the *Suzaku* observation. All reported uncertainties are at 90 per cent confidence level.

Parameter	HIGHECUT	NPEX	CUTOFFPL	COMPTT
$N_{\rm H1}^{a}$	$4.81^{+0.16}_{-0.22}$	$4.78^{+0.16}_{-0.20}$	$4.92^{+0.17}_{-0.21}$	$1.83^{+0.05}_{-0.04}$
$N_{\rm H2}^{a}$	$23.54^{+16.18}_{-10.23}$	$24.08^{+4.45}_{-4.51}$	$22.51^{+3.85}_{-4.01}$	$157.15^{+21.98}_{-23.44}$
CvrFract	$0.12^{+0.05}_{-0.04}$	$0.25^{+0.03}_{-0.03}$	$0.27^{+0.03}_{-0.03}$	$0.41^{+0.06}_{-0.07}$
PhoIndex	$0.77^{+0.05}_{-0.06}$	$0.58^{+0.10b}_{-0.09}$	$0.74^{+0.05}_{-0.06}$	–
Powerlaw(norm)[c]	$0.011^{+0.001}_{-0.001}$	$0.013^{+0.001}_{-0.001}$	$0.015^{+0.001}_{-0.001}$	–
Ecut (keV)	$5.94^{+0.23}_{-0.26}$	$12.26^{+2.49}_{-1.69}$	$18.06^{+2.20}_{-1.78}$	–
Efold (keV)	$19.21^{+2.17}_{-1.87}$	–	–	–
compTT (T_0) (keV)	–	–	–	$1.61^{+0.04}_{-0.04}$
compTT(kT) (keV)	–	–	–	$10.65^{+2.15}_{-1.13}$
compTT(taup)	–	–	–	$3.06^{+0.39}_{-0.53}$
compTT(norm)	–	–	–	$0.0056^{+0.0008}_{-0.0008}$
bbody(kT) (keV)	$0.137^{+0.007}_{-0.005}$	$0.138^{+0.006}_{-0.005}$	$0.134^{+0.006}_{-0.005}$	–
bbody(norm)[d]	$0.018^{+0.009}_{-0.007}$	$0.017^{+0.009}_{-0.006}$	$0.024^{+0.013}_{-0.009}$	–
Cyclabs[e] (keV)	$28.17^{+2.62}_{-3.36}$	$30.34^{+3.41}_{-5.79}$	$26.64^{+2.95}_{-3.95}$	$28.74^{+3.14}_{-2.93}$
Depth(keV)	$0.19^{+0.08}_{-0.08}$	$0.16^{+0.11}_{-0.09}$	$0.17^{+0.08}_{-0.07}$	$0.27^{+0.09}_{-0.08}$
Kα line (keV)	$6.42^{+0.01}_{-0.01}$	$6.42^{+0.01}_{-0.01}$	$6.42^{+0.01}_{-0.01}$	$6.42^{+0.01}_{-0.01}$
Equivalent width for Kα line (keV)	$0.029^{+0.004}_{-0.004}$	$0.029^{+0.003}_{-0.003}$	$0.029^{+0.003}_{-0.003}$	$0.029^{+0.003}_{-0.003}$
Kβ line (keV)	$7.09^{+0.03}_{-0.04}$	$7.12^{+0.03}_{-0.04}$	$7.13^{+003}_{-0.04}$	$7.08^{+0.01}_{-0.01}$
Equivalent width for Kβ line (keV)	$0.012^{+0.004}_{-0.004}$	$0.012^{+0.003}_{-0.003}$	$0.014^{+0.004}_{-0.004}$	$0.0029^{+0.004}_{-0.0028}$
$\rm Flux^{f}_{XIS}$	$1.57^{+0.04}_{-0.04}$	$1.56^{+0.02}_{-0.02}$	$1.51^{+0.04}_{-0.04}$	$1.52^{+0.04}_{-0.04}$
$\rm Flux^{f}_{HXD\text{-}PIN}$	$3.95^{+0.08}_{-0.08}$	$3.97^{+0.02}_{-0.02}$	$3.91^{+0.07}_{-0.07}$	$3.95^{+0.08}_{-0.08}$
χ^2_ν/d.o.f (with CYCLABS)	1.24/462	1.27/462	1.28/463	1.48/467
χ^2_ν/d.o.f (without CYCLABS)	1.28/464	1.29/464	1.32/465	1.55/469

Note.[a] In units of 10^{22} atoms $\rm cm^{-2}$.
[b] Photon index of the second power-law component of the NPEX is frozen to 2.0.
[c] In units of photons $\rm keV^{-1}$ $\rm cm^{-2}$ $\rm s^{-1}$ at 1 keV.
[d] In units of L_{39}/D_{10}.
[e] Width frozen at 9.8 keV (Bonning & Falanga 2005).
[f] In units of 10^{-10} erg $\rm cm^{-2}$ $\rm s^{-1}$.

To determine the orbital phase of the *Suzaku* observation, we folded the *Suzaku*-XIS and HXD-PIN light curves together with the *Swift*-BAT[4] and *RXTE*-ASM[5] long-term light curve of 4U 0114+65 at an orbital period of 11.596 d. The latter was obtained from the *RXTE*-ASM light curve using the FTOOLS task 'EFSEARCH'. The folded light curves in Fig. 2 clearly show that the *Suzaku* observation was carried out during the X-ray dip.

We also extracted the energy resolved pulse profiles of the source, normalized at the average source intensity for the XIS and HXD-PIN data. As shown in Fig. 3, the profiles do not show any significant energy dependence and pulsations are always detected up to 70 keV.

2.1.2 *Spectral analysis*

We performed a time-averaged spectral analysis of the X-ray emission from 4U 0114+65 using the two XIS units (XIS 0 and 3) and the HXD-PIN data. Data from the BI XIS 1, were not included in the spectral analysis as the cross-normalizations obtained between the XIS 0 and the XIS 1 were larger than those suggested in the *Suzaku* ABC guide. Additionally, we also noticed systematic differences in the spectral fitting of the BI data compared to the other XIS units. Such differences between the BI and FI XIS units have been previously reported, e.g. in the case of GX 301-2 (Suchy et al. 2012) and IGR J16318−4848 (Barragán et al. 2009). In these situations, it is more convenient to use only the data from the FI XIS units, given the greater sensitivity of the latter chips above 2 keV compared to the BI XIS unit.

Spectral fitting was performed by using XSPEC v12.8.2. For the spectral analysis, we have chosen the energy range 0.8–10 keV for the XIS units and 15.0–70.0 keV for the HXD-PIN, respectively. Artificial residuals are known to arise in the XIS spectra around the Si edge and Au edge. The energy range 1.75–2.23 keV is thus usually discarded for the spectral analysis. We fitted all spectra simultaneously with all parameters tied, except the relative instrument normalizations which were kept free to vary. The 2048 channel XIS spectra were rebinned by a factor of 6 up to 5 keV, by a factor of 2 from 5–7 keV, and by a factor of 14 in the remaining energy range. The HXD-PIN spectra were binned by a factor of 4 at energies $\leq$22 keV, by 8 in the energy range 22–45 keV, and by 12

[4] http://swift.gsfc.nasa.gov/results/transients/weak/3A0114p650/
[5] ftp://legacy.gsfc.nasa.gov/xte/data/archive/ASMProducts/definitive_1dwell/lightcurves/

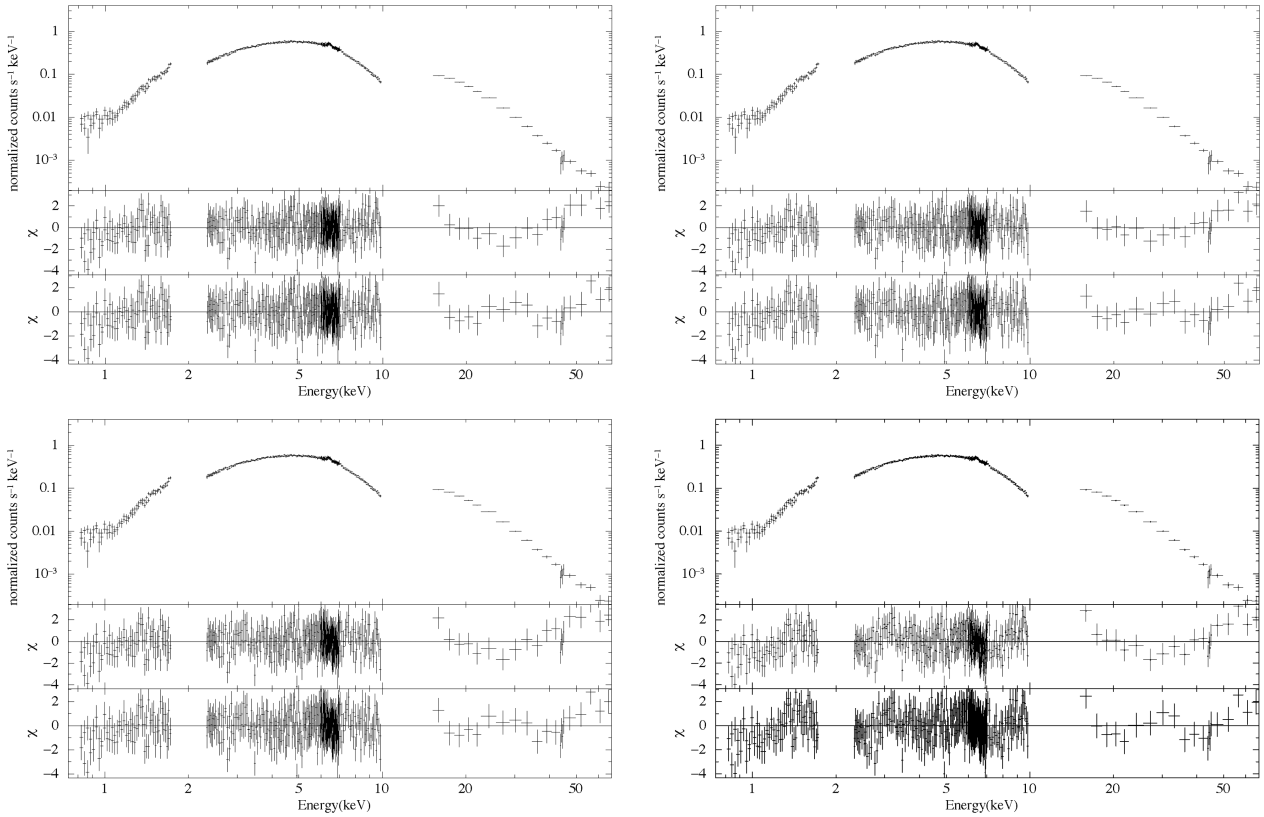

Figure 4. Time-averaged X-ray spectra of 4U 0114+65 for *Suzaku*-XIS and HXD-PIN data of 4U 0114+65 fitted with the four models measured in the text. The second panel in each figure shows the residuals from the fits when the cyclotron absorption component is not included. The third panel represents the same residuals after the inclusion of the absorption feature. The model used for upper left fitting is HIGHECUT, upper right is NPEX, lower left is CUTOFFPL and lower right is COMPTT.

in the remaining part of the instrument passband. To fit the spectral continuum, we used the continuum models commonly used for HMXBs, such as a power-law model modified with an exponential cutoff (CUTOFFPL), a power law with a high energy cutoff (HIGHECUT; White, Swank & Holt 1983; Heindl et al. 2001), a negative and positive power law with exponential continuum model (NPEX; Mihara 1995; Makishima et al. 1999) and a physical Comptonization model (COMPTT; Titarchuk 1994). In addition to the interstellar absorption along our line of sight, we also used a partial covering component to account for local absorption. A soft excess below 2 keV remained visible in the residuals from the fits with all above models except COMPTT. Where significantly detected, the soft excess was accounted for with the addition of a blackbody component. Two Gaussian components were added to fit the iron Kα and Kβ emission lines. An evident feature is seen in the residuals from all the fits between 20 and 30 keV, irrespective of the model used for the continuum. The inclusion of an absorption cyclotron feature (CYCLABS) with a width fixed at 9.8 keV (Bonning & Falanga 2005) slightly improved the fit. To test further, the significance of the cyclotron line detected, we used the *F*-test routine available in the IDL package mpftest[6] (DeCesar et al. 2013). The probability of chance improvement (PCI) is evaluated for the HIGHECUT model used to fit the spectrum with and without the cyclotron line. The estimated PCI value after addition of cyclotron line component to the HIGHECUT is ∼38.4 per cent. The best-fitting spectral parameters for 4U 0114+65 for all considered models are summarized in Table 1. The time-averaged spectra for different models and their residuals with and without the inclusion of the CYCLABS component are shown in Fig. 4. At energies above 50 keV, the residuals also suggested the presence of a high energy tail in 4U 0114+65 (den Hartog et al. 2006; Wang 2011), the detailed fitting of which we have not been able to carry out since the HXD-PIN spectrum is limited to 70 keV.

To perform a time-resolved spectral analysis of the emission within the dip, we divided the light curve into 14 segments. Each segment is defined to be the time elapsed between two successive minima in the light curve, as is depicted in Fig. 1. This way, the average time interval between the segments turn out to be ∼9355 s, which is nearly equal to the spin period of the pulsar (∼9391 s).

The time-resolved spectra (shown in Fig. 5) could be well fit with the HIGHECUT model, which also provided the best description of the time-averaged spectrum. The variations of the spectral parameters with time obtained for the HIGHECUT model are shown on the left-hand side of Fig. 6.

For the spin-phase-resolved spectral analysis, we extracted the source spectra in 16 phase bins. Each phase-resolved spectrum was again fitted with the HIGHECUT model. The variation of the spectral parameters with the spin phase is shown on the right-hand side of Fig. 6.

From the time-resolved spectral analysis of the source, we obtained the following results.

(i) The partial covering absorption component was not needed to fit the time-resolved spectra. The measured variation of $N_{\rm H}$ with time

[6] http://www.physics.wisc.edu/~craigm/idl/down/mpftest.pro

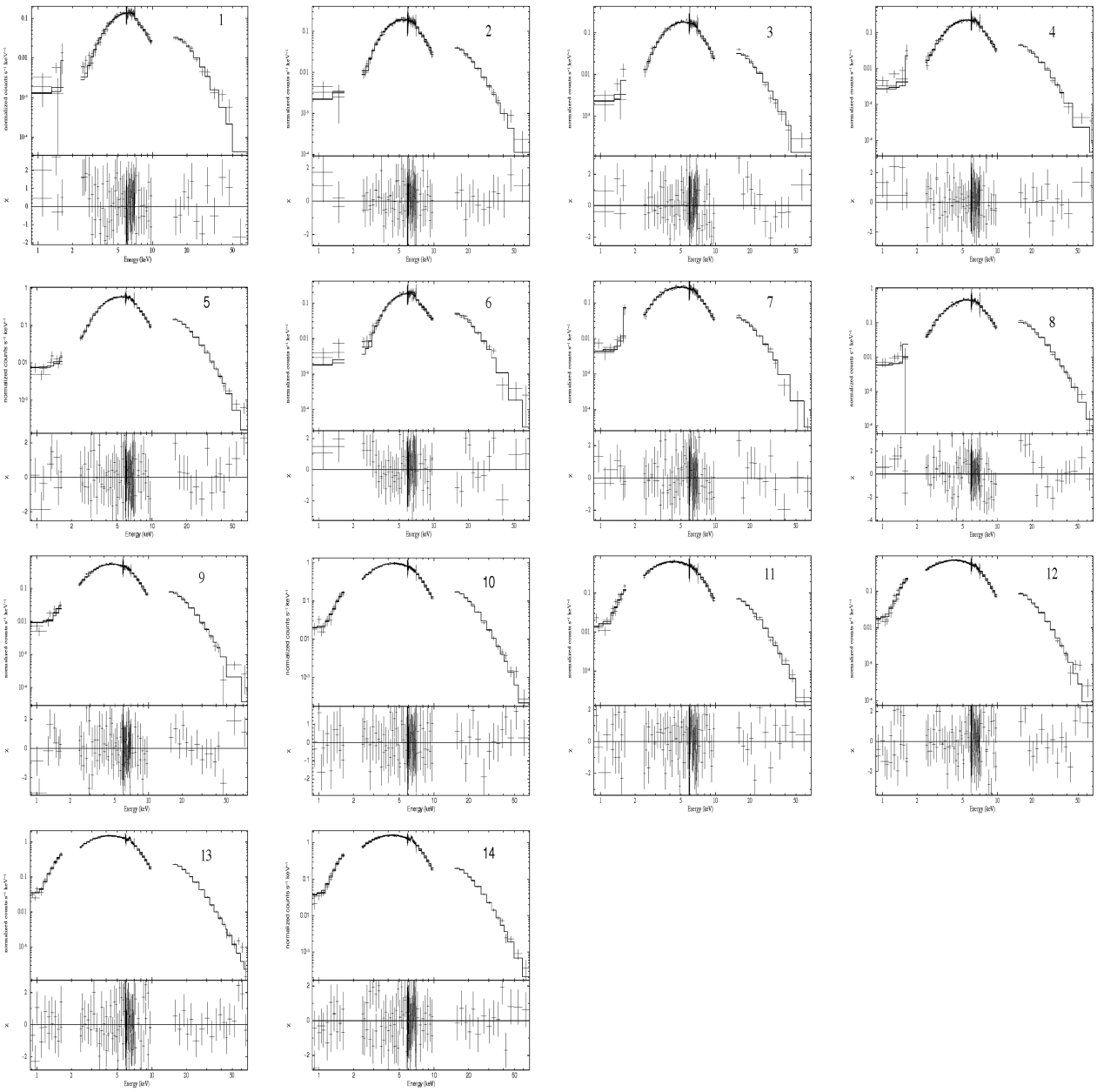

Figure 5. Time-resolved spectra of 4U 0114 +65 fit with the HIGHECUT model. Residuals from the fits are shown in the bottom panel of each figure.

suggests the presence of clumps in the neutron star surroundings as in the case of GX 301-2 (Mukherjee & Paul 2004), Vela X-1 (Fürst et al. 2010), Cen X-3 (Naik, Paul & Ali 2011) and OAO 1657-415 (Pradhan et al. 2014). We found that the $N_{\rm H}$ was higher at the beginning of the observation (2×10^{23} atoms cm^{-2}) and decreased by a factor of 10 towards the end of the *Suzaku* observation window.

(ii) For low-flux segments like (2–5 and 7–8 and 12), the blackbody temperature had to be frozen to the time-averaged value while allowing the blackbody normalization to vary. For low-flux segments 1 and 6, we could not constrain the blackbody normalization even by freezing the blackbody temperature to time-averaged value.

(iii) Residuals from the fits around the cyclotron line energy are not detected in most of the time-resolved segments (due to low statistics) except for the segments 3, 5 and 8. In these cases, however, the statistics was far too low to perform a meaningful test about the statistical significance of the possible cyclotron line.

From the results of the phase-resolved spectral analysis, we conclude the following.

(i) As for the time-resolved spectral analysis, the partial covering absorption component was not required to fit the phase-resolved spectra.

(ii) Only the photon index and the normalization of the power-law component show some moderately significant variability with the pulse phase.

(iii) Residuals around the energy of the cyclotron line could not be detected, most likely due to the limited statistics compared to the phase-averaged spectrum.

Finally, we showed through our timing analysis of the *Suzaku* data that pulsations are detected in the X-ray emission of the source also during the time interval corresponding to the dip.

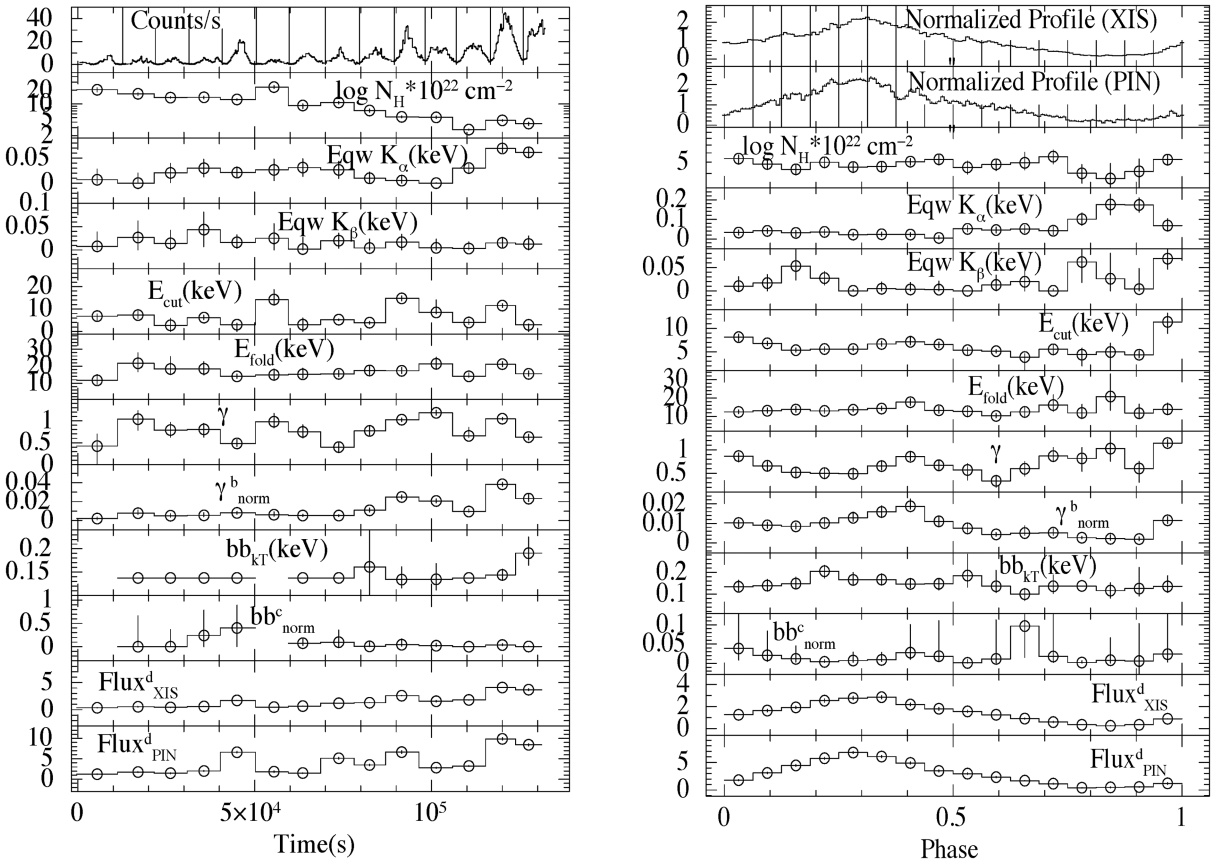

Figure 6. Left: variations of the source spectral parameters (for the HIGHECUT model) with time ($t = 0$ corresponds to MJD 55763.4805). Right: variations of the source spectral parameters with pulse phase (for the HIGHECUT model). ^{b} = In units of photons keV^{-1} cm^{-2} s^{-1} at 1 keV, ^{c} = In units of L_{39}/D_{10}; ^{d} = In units of 10^{-10} erg cm^{-2} s^{-1}.

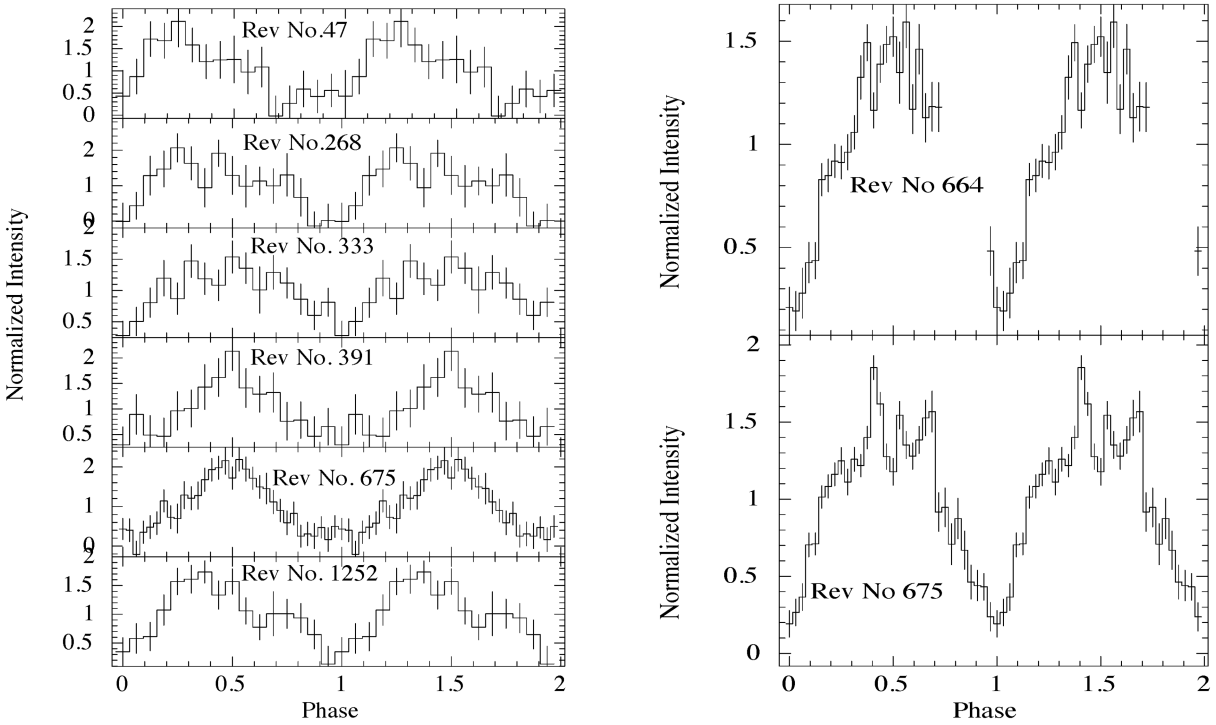

Figure 7. Left: pulse profiles extracted from the IBIS/ISGRI data (20–40 keV). Right: pulse profile extracted from the JEM-X data (3–35 keV). In both panels, the epoch chosen for the folding is arbitrary.

2.2 *INTEGRAL*/IBIS and JEM-X light curves

We used all publicly available *INTEGRAL* data collected in the direction of 4U 0114+65 since the earliest science operations of the mission. This data set comprises 'science windows' (SCWs), i.e. pointings with typical durations of ∼2–3 ks, carried out from the satellite revolution 25 to 1471. We analysed all data from the IBIS/ISGRI (Lebrun et al. 2003) and the two JEM-X (Lund et al. 2003) instruments by using version 10.1 of the Off-line Scientific Analysis software (OSA) distributed by the ISDC (Courvoisier et al. 2003). To limit the IBIS/ISGRI calibration uncertainties, we selected only SCWs during which the source was located to within 12° from the centre of the IBIS Field Of View (FoV) (Ubertini et al. 2003). The total effective exposure time was of 8.9 Ms for IBIS/ISGRI, 1.4 Ms for JEM-X1, and 520 ks for JEM-X2. From all the available *INTEGRAL* IBIS/ISGRI and JEM-X observations of 4U 0114+65, we extracted the source light curves with a time binning of 100 s in the energy range 20–40 keV and 3–35 keV, respectively. We then searched for pulsations during those observations that were carried out at orbital phases corresponding to the X-ray dip (±1 d). Except for those cases where the statistics of the data was relatively low, pulsations were seen in most of the observations and a few examples of pulse profiles are shown in Fig. 7.

3 DISCUSSION

In this paper, we used *Suzaku* and *INTEGRAL* data to study the X-ray emission from 4U 0114+65 during the orbital phase corresponding to its periodic X-ray dip. Such dip has been interpreted in the past as an eclipse of the neutron star hosted in this system by its supergiant companion. However, our analysis revealed some anomalous properties of the source X-ray emission that would not support such interpretation. In particular we noted the following.

(i) The orbital intensity profile of 4U 0114+65 in the proximity of the X-ray dip is different from that of other eclipsing HMXBs which typically show sharp eclipse ingresses and egresses in hard X-rays and a more gradual variation of their intensity in soft X-rays owing to absorption in the stellar wind. On the contrary, we showed that 4U 0114+65 exhibits an eclipse-like profile at the lower energies (*RXTE*-ASM) with the ingress and egress time of the dip being nearly a day-long each, and a more gradual variation in hard X-rays (*Swift*-BAT).

(ii) The X-ray spectra of HMXBs during eclipses are characterized by the presence of prominent iron lines with large equivalent widths, (see e.g. the cases of Vela X-1, Nagase et al. 1994; Cen X-3, Nagase et al. 1992; Naik et al. 2011). The spectrum of 4U 0114+65 does not show such feature.

(iii) The spectral index during eclipse should be higher than out of eclipse phases, since during eclipse, we will be observing only the scattered emission in the wind. As an example, in the *Suzaku* observation of Cen X-3 when the pulsar was observed during eclipse and out of eclipse phases, the photon index correlates well with those orbital phases (fig. 6 of Naik et al. 2011). We see no such correlation here.

(iv) Eclipse ingresses and egresses of HMXBs are often characterized by extremely large increases/decreases of the absorption column densities due to the presence of the dense wind of the supergiant star along the line of sight to the observer ($N_{\rm H} \geq 10^{24}$ atoms cm^{-2}). A soft excess should not be observable in these cases, as the X-ray emission at energies ≤2 keV is strongly extinguished. In the case of 4U 0114 +65, we observe only a moderate increase of the absorption column density in the dip compared to other orbital phases and also the soft excess below ∼2 keV remains clearly detectable in the averaged *Suzaku* spectrum and in those segments where the flux is not too low.

(v) Pulsations were clearly detected during all available *INTEGRAL* observations carried out during the X-ray dip and the *Suzaku* observations, even though in these cases the source was supposed to be in eclipse.

Different works in the past have investigated the origin of the X-ray dip in 4U 0114+65. Hall et al. (2000) and Corbet et al. (1999) reported a definite truncation of X-ray signal near orbital phase 0 indicative of an eclipse which is further supported by an increase in column density near the same phase (Hall et al. 2000). On the other hand, neither Crampton et al. (1985) nor Farrell et al. (2008) found convincing evidence for the presence of an X-ray eclipse in the *RXTE*/PCA and optical data. Grundstrom et al. (2007) was the first to note that the minimum in the X-rays occurs very close to the predicted phase of the supergiant inferior conjunction. In agreement with their findings, we thus propose that, as the system is characterized by an eccentric orbit, the accretion rate on to the neutron star is modulated along the orbital phase, leading to variations in both soft and hard X-rays. It is not an eclipsing binary, but at the inferior conjunction of the companion star, increased absorption in the stellar wind causes a dip in the soft X-ray orbital light curve, which is also seen in the form of a larger $N_{\rm H}$ in the beginning of the *Suzaku* observation. It shall be remarked that the detection of X-ray pulsations during the dip cannot be used to distinguish between the idea proposed above and the eclipse model. Indeed, the long spin period of the pulsar hosted in 4U 0114+65 would allow us to detect pulsations even when the source is eclipsed, as these would not be washed out in the emission reprocessed by the stellar wind.

Finally, we suggest that the variations of the absorption column density (see Fig. 6) recorded during the *Suzaku* observation on time-scales of few thousand seconds might be due to the presence of clumps in the wind of the supergiant companion as observed also in other similar systems (see e.g. GX 301-2, Vela X-1, Cen X-3 and OAO 1657-415; Mukherjee & Paul 2004; Fürst et al. 2010; Naik et al. 2011; Pradhan et al. 2014; Walter et al. 2015).

ACKNOWLEDGEMENTS

This research has made use of data obtained from the *Suzaku* satellite, a collaborative mission between the space agencies of Japan (JAXA) and the USA (NASA). The data for this work have been obtained through the High Energy Astrophysics Science Archive (HEASARC) Online Service provided by NASA/GSFC. We have also made use of public light curves from *Swift* and *RXTE* site. PP is thankful to University Grants Commission (UGC), India for their financial support under 'Minor Research Project' and also to the hospitality provided by Raman Research Institute, Bangalore for carrying out this work. TMB acknowledges support from INAF-PRIN 2012-6. The authors would also like to thank the anonymous referee for the useful comments and suggestions.

REFERENCES

Apparao K. M. V., Bisht P., Singh K. P., 1991, ApJ, 371, 772
Barragán L., Wilms J., Pottschmidt K., Nowak M. A., Kreykenbohm I., Walter R., Tomsick J. A., 2009, A&A, 508, 1275
Bonning E. W., Falanga M., 2005, A&A, 436, L31
Corbet R. H. D., Finley J. P., Peele A. G., 1999, ApJ, 511, 876
Courvoisier T. J.-L. et al., 2003, A&A, 411, L53

Crampton D., Hutchings J. B., Cowley A. P., 1985, ApJ, 299, 839
DeCesar M. E., Boyd P. T., Pottschmidt K., Wilms J., Suchy S., Miller M. C., 2013, ApJ, 762, 61
den Hartog P. R., Hermsen W., Kuiper L., Vink J., in't Zand J. J. M., Collmar W., 2006, A&A, 451, 587
Dower R., Kelley R., Margon B., Bradt H., 1977, IAU Circ., 3144, 2
Farrell S. A., Sood R. K., O'Neill P. M., 2006, MNRAS, 367, 1457
Farrell S. A., Sood R. K., O'Neill P. M., Dieters S., 2008, MNRAS, 389, 608
Finley J. P., Belloni T., Cassinelli J. P., 1992, A&A, 262, L25
Fukazawa Y. et al., 2009, PASJ, 61, 17
Fürst F. et al., 2010, A&A, 519, A37
Grundstrom E. D. et al., 2007, ApJ, 656, 431
Hall T. A., Finley J. P., Corbet R. H. D., Thomas R. C., 2000, ApJ, 536, 450
Heindl W. A., Coburn W., Gruber D. E., Rothschild R. E., Kreykenbohm I., Wilms J., Staubert R., 2001, ApJ, 563, L35
Koenigsberger G., Swank J. H., Szymkowiak A. E., White N. E., 1983, ApJ, 268, 782
Koyama K. et al., 2007, PASJ, 59, 23
Lebrun F. et al., 2003, A&A, 411, L141
Li X.-D., van den Heuvel E. P. J., 1999, ApJ, 513, L45
Lund N. et al., 2003, A&A, 411, L231
Makishima K., Mihara T., Nagase F., Tanaka Y., 1999, ApJ, 525, 978
Masetti N., Orlandini M., dal Fiume D., del Sordo S., Amati L., Frontera F., Palazzi E., Santangelo A., 2006, A&A, 445, 653
Mihara T., 1995, PhD thesis, Univ. Tokyo
Mitsuda K. et al., 2007, PASJ, 59, 1
Mukherjee U., Paul B., 2004, A&A, 427, 567
Nagase F., Corbet R. H. D., Day C. S. R., Inoue H., Takeshima T., Yoshida K., Mihara T., 1992, ApJ, 396, 147
Nagase F., Zylstra G., Sonobe T., Kotani T., Inoue H., Woo J., 1994, ApJ, 436, L1
Naik S., Paul B., Ali Z., 2011, ApJ, 737, 79
Pradhan P., Maitra C., Paul B., Islam N., Paul B. C., 2014, MNRAS, 442, 2691
Reig P., Chakrabarty D., Coe M. J., Fabregat J., Negueruela I., Prince T. A., Roche P., Steele I. A., 1996, A&A, 311, 879
Sood R., Farrell S., O'Neill P., Manchanda R., Ashok N. M., 2006, Adv. Space Res., 38, 2779
Suchy S., Fürst F., Pottschmidt K., Caballero I., Kreykenbohm I., Wilms J., Markowitz A., Rothschild R. E., 2012, ApJ, 745, 124
Takahashi T. et al., 2007, PASJ, 59, 35
Taylor M., Finley J. P., Kurt C., Koenigsberger G., 1995, AJ, 109, 396
Titarchuk L., 1994, ApJ, 434, 570
Ubertini P. et al., 2003, A&A, 411, L131
Walter R., Lutovinov A. A., Bozzo E., Tsygankov S. S., 2015, A&AR, 23, 2
Wang W., 2011, MNRAS, 413, 1083
Wen L., Levine A. M., Corbet R. H. D., Bradt H. V., 2006, ApJS, 163, 372
White N. E., Swank J. H., Holt S. S., 1983, ApJ, 270, 711
Yamauchi S., Asaoka I., Kawada M., Koyama K., Tawara Y., 1990, PASJ, 42, L53

This paper has been typeset from a TEX/LATEX file prepared by the author.